Cardiovasc Intervent Radiol
https://doi.org/10.1007/s00270-024-03813-x

Transarterial Embolization Enhances Programmed Cell Death Ligand 1 Expression and Influences CD8$^+$T Lymphocytes Cytotoxicity in an Orthotopic Hepatocellular Carcinoma Rat Model

Shen Zhang[1] · Lin Xu[1] · Jia-Qing Li[1] · Ming-Zhan Du[2] · Yu Yin[1] · Bin-Yan Zhong[1] · Han-Si Liang[3] · Wan-Ci Li[1] · Cai-Fang Ni[1] · Xiao-Li Zhu[1]

Received: 19 November 2023 / Accepted: 10 July 2024

Abstract

Purpose To investigate the influence of transarterial embolization (TAE) on programmed cell death-ligand 1(PD-L1) expression and CD8$^+$T tumour infiltrative lymphocyte cytotoxicity in the Sprague–Dawley (SD) rat model of hepatocellular carcinoma (HCC).

Materials and Methods An orthotopic HCC model was established in twenty SD rats treated with TAE (lipiodol, n = 10) or sham (normal saline, n = 10) using homologous N1S1 hepatoma cells. Rats were euthanized 1 week after embolization. Flow cytometry was used to assess the proportion of CD4$^+$T, CD8$^+$T and programmed cell death-1$^+$(PD-1$^+$) CD8$^+$T lymphocytes in the spleens and tumours. Distribution of CD8$^+$T, granzyme-B$^+$CD8$^+$T lymphocytes and PD-L1$^+$ cells was assessed by immunohistochemistry (IHC) or multiplex IHC. p value < 0.05 was considered statistically significant.

Results The CD4/CD8 ratio and PD-1$^+$CD8$^+$ T lymphocytes exhibited higher values in TAE-treated tumours compared to sham-treated tumours ($p = 0.021$ and $p = 0.071$, respectively). Conversely, the number of CD8$^+$T lymphocytes was decreased in TAE-treated tumours ($p = 0.043$), especially in the central region ($p = 0.045$). However, more CD8$^+$T lymphocytes were found infiltrating the marginal region than central region in TAE-treated tumours ($p = 0.046$). The proportion of granzyme-B$^+$CD8$^+$T lymphocytes and the PD-L1 positive areas was elevated in tumours that treated with TAE (p all < 0.05). There was a negative correlation between PD-L1 expression and the number of infiltration of CD8$^+$ T lymphocytes ($p = 0.036$).

Conclusions Immune cells are distributed unevenly in the tumours after TAE. The intrinsic induction state of the tumour after embolization may be insufficient to elicit a maximal response to PD-1/PD-L1 inhibitors.

Shen Zhang, Lin Xu and Jia-Qing Li have contributed to this equally.

✉ Xiao-Li Zhu
zhuxiaoli90@163.com

[1] Present Address: Department of Interventional Radiology, The First Affiliated Hospital of Soochow University, No. 899, Pinghai Road, Suzhou 215006, China

[2] Department of Pathology, The First Affiliated Hospital of Soochow University, Suzhou, China

[3] Jiangu Institute of Clinical Immunology, The First Affiliated Hospital of Soochow University, Suzhou, China

Published online: 05 August 2024

Graphical Abstract

CVIR The official journal of the Cardiovascular and Interventional Radiological Society of Europe
CardioVascular and Interventional Radiology
Springer CIRSE

Transarterial Embolisation Enhances Programmed Cell Death Ligand 1 Expression and Influences CD8⁺T Lymphocytes Cytotoxicity in An Orthotopic Hepatocellular Carcinoma Rat Model

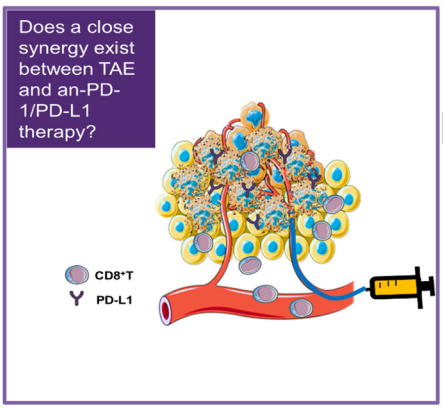

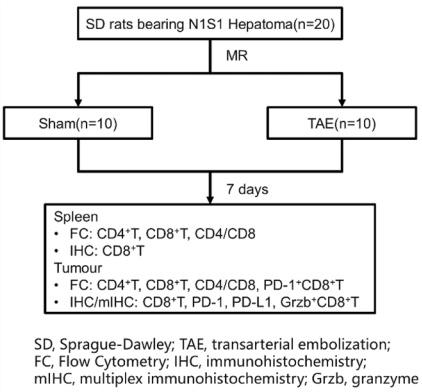

Groups	Parameters	Values(% or count/mm²)	p-value[a]
TAE vs. Sham	CD4/CD8	0.89 ± 0.16 vs. 0.71 ± 0.15	**0.021**
	CD8⁺T	113 ± 16 vs. 128 ± 13	**0.043**
	PD-1⁺CD8⁺T	23.49 ± 7.20 vs. 18.12 ± 4.33	0.071
	Grzb⁺CD8⁺%	30.09 ± 7.70 vs. 22.20 ± 4.17	**0.015**
	PD-1	7.65 ± 0.86 vs. 6.86 ± 0.95	0.08
	PD-L1	18.67 ± 5.43 vs. 13.59 ± 2.18	**0.002**

PD-1, programmed cell death-1;
PD-L1, programmed cell death ligand-1;
Grzb, granzyme-B;
TAE, transarterial embolization;
p-value[a] calculated using Student's t-test or the Mann-Whitney U test

Keywords Hepatocellular carcinoma · Transarterial embolization · Tumour immune microenvironment · Programmed cell death ligand 1 · $CD8^+$T lymphocytes

Introduction

The highly heterogeneous nature of hepatocellular carcinoma (HCC) results in the long-term efficacy of transarterial chemoembolization (TACE) being less than optimal [1, 2]. Fortunately, the advent of immune checkpoint inhibitors (ICIs) rekindles optimism to the field of TACE combination therapy based on the hypothesis that locoregional treatment could prompt immunogenic cell death [3–7]. Nevertheless, the impact of TACE on the tumour immune microenvironment (TIME), as well as the potential for synergy between TACE and ICIs, remains to be investigated.

The intricate interrelationships between tumour cells, immune cells, cytokines and other elements constitute the cancer-immunity cycle. Given that the immune landscape of the peripheral and tumour microenvironment may differ, the reconstruction of TIME following TACE, through the monitoring of immune indexes in peripheral blood, may be inaccurate, and indeed, conflicting [8–10]. The $CD8^+$T lymphocytes, a type of cytotoxic T lymphocytes (CTLs), play a pivotal role in anti-tumour immunity. The infiltration of $CD8^+$T lymphocytes and the expression of programmed cell death ligand-1(PD-L1) have been utilized as biomarkers for characterizing tumour immunotypes and predicting ICIs response [11]. It is noteworthy that existing studies concerning TACE have not accorded sufficient attention to these two indicators, and the varying intervals between TACE and surgery have yielded conflicting results [12–14]. Montasser et al. suggested that chemoembolization-induced PD-L1 elevation may enhance the tumours response to ICIs [13]. However, Craciun et al. disagreed as TACE was incapable of enhancing $CD8^+$T lymphocytes infiltration in tumours[12]. Contradictorily, Pinato et al. proposed that TACE reduced the number of $CD8^+$T lymphocytes, yet did not affect PD-L1 expression [14]. While experimental animal studies overcame the heterogeneity of observation periods and revealed the potential synergy between transarterial embolization (TAE) and ICIs, further research is warranted to elucidate the characteristics of $CD8^+$T lymphocytes [15, 16]. The activated $CD8^+$T lymphocytes, which express granzyme-B or IFN-γ, and the exhausted subsets, which overexpress immune checkpoints such as programmed cell death-1(PD-1), display distinct immune properties.

The objective of this animal study is to further investigate the influence of embolization on TIME, with the aim

of assessing the potential value of arterial embolization in combination with anti-PD-1/PD-L1. This will be achieved by examining the alteration of $CD8^+$T lymphocytes, including their subtypes, as well as PD-1/PD-L1 expression.

Material and Methods

Experimental Design

N1S1 rat hepatocellular carcinoma cells were obtained from ATCC (CRL-1601, ATCC, Manassas, USA). Adult male Sprague–Dawley (SD) rats aged between 8 and 12 weeks were employed in this study. All animal experiments followed the basic guidelines for animal experiments and related activities and received approval from the Institutional Animal Care and Use Committee. After anesthetizing with 1% pentobarbital sodium liquid, a mixture of approximately 50 µl of phosphate-buffered saline (PBS) containing 3–3.5 $\times$ 10^6 N1S1 cells was slowly injected into the subcapsular area of the left hepatic lobe during a midline mini-laparotomy. T2-weighted magnetic resonance imaging (MRI) was performed on anesthetized animals using a 3.0-T MRI scanner (GE, Connecticut, USA) 7 days after laparotomy to identify the tumour node and verify its diameter exceeded 0.5 cm (Fig. S1a). The rats were subsequently assigned to TAE (lipiodol, n = 10) and sham groups (normal saline, n = 10) with simple randomization. Strict standards were designed to prevent potential bias from spontaneous tumour regression [17]. The resource equation approach governed the minimum of six rats per group (detail information seeing in *Supplementary material*).

Image-guided intra-arterial embolization

TAE was performed the next day of MRI scanning. Rat caudal artery was exposed and then punctured with a 26-gauge needle, followed by insertion of a 1.7F SL-10 microcatheter (Stryker, Michigan, USA) accompanied by a matched guidewire. The microcatheter was advanced to the distal portion of the hepatic artery as far as possible under fluoroscopic guidance (Fig. S1b). The rats in the sham group received an injection of 0.2 ml of normal saline, while those in the TAE group were administrated with lipiodol until the blood flow was considerably slowed down. Afterwards, a minute quantity of 100-300 µm of gelatin sponge particles (Alicorn, Zhejiang, China) was introduced until the blood flow reached stasis (Fig. S1c).

Histopathologic Analysis

All animals were euthanized and their organs were harvested 7 days after embolization. One 4-µm-thick paraffin section included whole tumour was stained with hematoxylin and eosin (Fig. S1d). Immunohistochemistry (IHC) or multiplex IHC (mIHC) staining was conducted for $CD8^+$T, granzyme-B^+CD8^+T lymphocytes and PD-1^+/PD-$L1^+$ cells. The tyramide signal amplification technique was employed for the mIHC procedure (detailed process and antibody information were presented in *Supplementary Material*).

Flow Cytometry

Fresh spleen and tumour samples were immediately transferred to cold PBS-2% fetal bovine serum for flow cytometric (FCM) analysis, including $CD4^+$T, $CD8^+$ T and PD-1^+CD8^+T lymphocyte count and determination of theCD4/CD8 ratio. Cells were collected using a Beckman flow cytometer (Beckman Coulter, Indiana, USA) and data were further analysed using FlowJo v10 (Tree Star Inc). Detailed protocol was presented in *Supplementary Material.*

Cell counting and Image analysis

For (m)IHC sections, target cells were identified and quantified via automatic recognition using inform 2.6.0 software (Akoya, MA, USA) following pre-training for cell segmenting and phenotyping (Fig. S2a, S2b). Subsequently, two independent pathologists (MZ D and HS L) re-validated the results to ascertain the reliability of the automated process. Should both pathologists deemed that the machine recognition error was substantial upon visual examination, the image would be re-analysed or altered. Positive cells situated in the three central regions (which constitutes approximately half of the tumour volume) and in three marginal regions (areas outside of the centre) were enumerated and analysed separately, with necrotic areas excluded to the greatest extent possible. The average number of $CD8^+$T lymphocytes, as well as those expressing granzyme-B staining, was quantified as cells per square millimetre. Besides, the average percentage of the defined region that was positively stained for PD-1 and PD-L1 was scored.

Statistical Analysis

Statistical analyses were performed with GraphPad Prism v8.0.2 software (San Diego, CA, USA). Data were

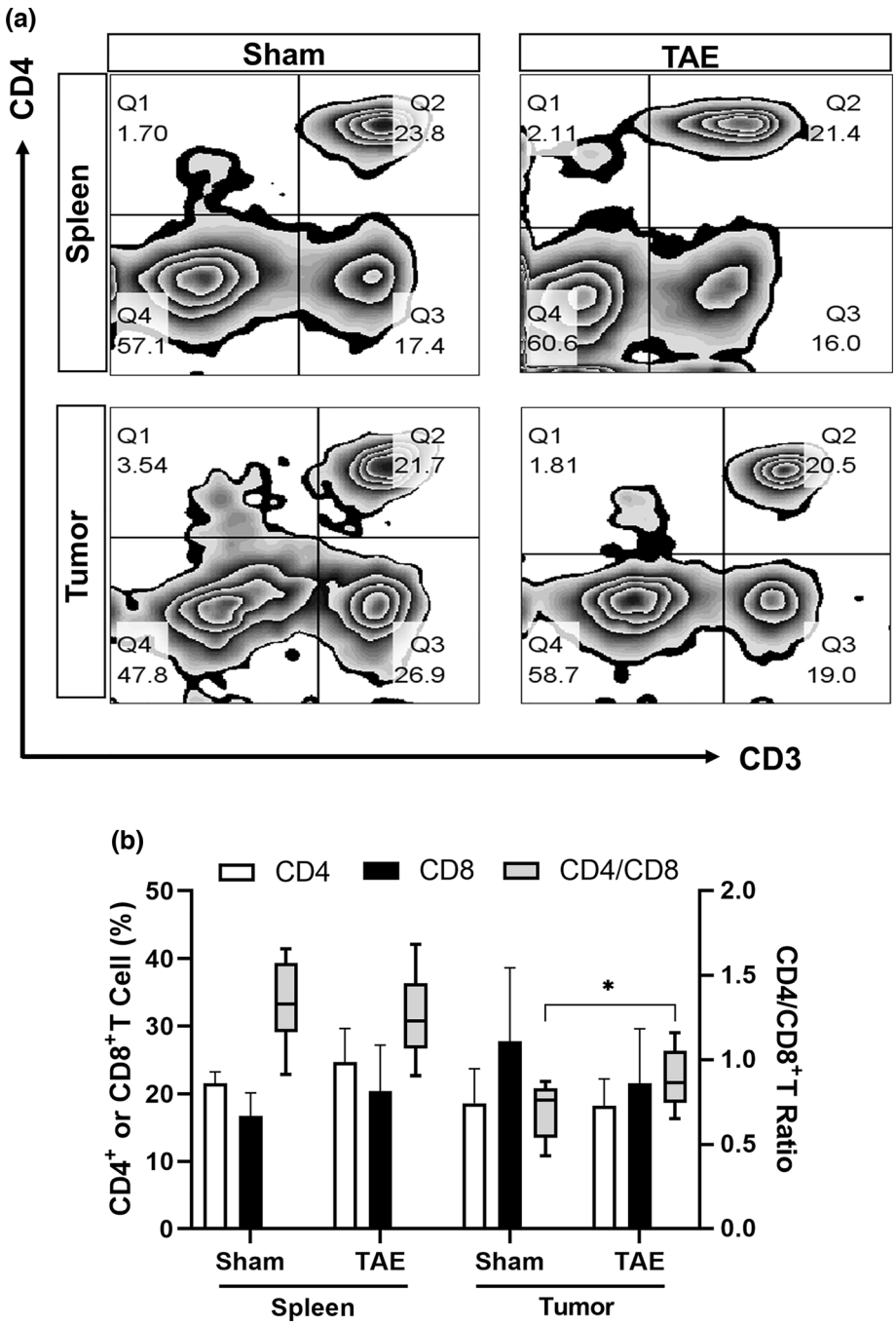

Fig. 1 The frequency of $CD8^+$T and $CD4^+$T lymphocytes in spleen and tumour tissues by flow cytometry (FCM). **a** Representative FCM contour plots indicate no significant differences in the proportion of $CD4^+$T and $CD8^+$T lymphocytes in tumour or spleen tissues in TAE (n = 10) or sham (n = 10) group. **b** Quantitative analysis illustrates an increased CD4/CD8 ratio in TAE-treated tumour tissue compared with sham embolization. $*p < 0.05$

presented as mean ± standard error of the mean. Statistical comparisons of data were conducted using the Student's t test or the Mann–Whitney U test. The correlation test was undertaken by Pearson correlation coefficient. All test results were considered statistically significant when $p < 0.05$.

Results

TAE Increased CD4/CD8 Ratio and Decreased $CD8^+$T Lymphocytes Infiltration in Tumour

There were no discernible differences in the proportion of $CD4^+$T or $CD8^+$T in the spleen or tumour between TAE-treated and sham-treated rats (Table S1, Fig. 1a, 1b). Notably, the CD4/CD8 ratio was increased in the TAE-treated tumours compared with the sham-treated tumours

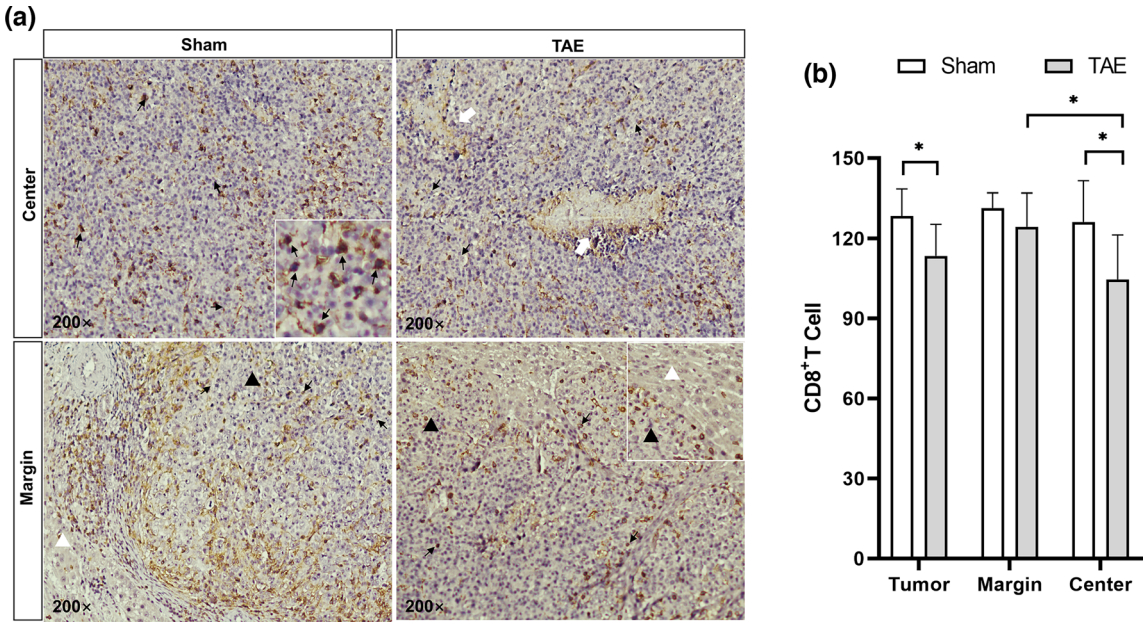

Fig. 2 The profile of $CD8^+T$ lymphocytes infiltrating in tumour centre and tumour margin by immunohistochemistry (IHC). **a** $CD8^+T$ lymphocytes (black arrows) infiltrate the tumour tissue extensively, with a higher abundance of $CD8^+T$ at the tumour marginal regions. **b** Quantitative analysis demonstrates a reduction in $CD8^+T$ lymphocytes in TAE-treated tumour, with a particularly significant differences in tumour central regions. The number of $CD8^+T$ lymphocytes in TAE-treated group is higher at the margin of tumours than in the centre. $*p < 0.05$. White bold arrows, necrosis; black triangle, tumour tissue; white triangle, normal liver tissue

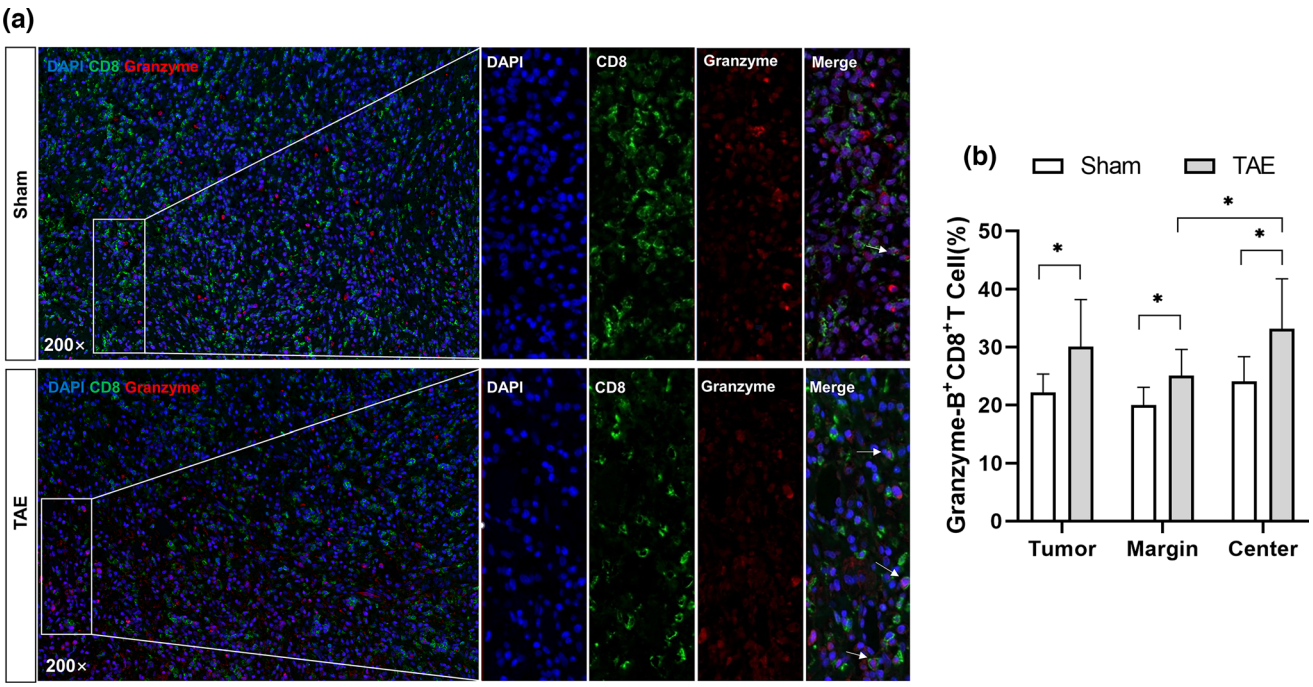

Fig. 3 Characterization of the expressions and localizations of $CD8^+T$ lymphocytes and granzyme-B^+ lymphocytes in tumour tissues by multiple IHC. **a** An enlarged subsection of the composite fluorescent image is highlighted to demonstrate granzyme$^+CD8^+T$ lymphocytes (two rightmost images, white arrows) and each individual markers, including the DAPI nuclear marker (nucleus, pseudo-coloured blue), $CD8^+T$ (membrane, pseudo-coloured green), granzyme-B^+ cell (cytoplasm, pseudo-coloured red) and the autofluorescence signal (pseudo-coloured black) at 200 × magnification. **b** Quantitative analysis shows a higher number of granzyme-B^+CD8^+T lymphocytes in TAE-treated tumour. The percentage of the granzyme-B^+CD8^+T lymphocyte subset is higher in the TAE-treated tumour, particularly in the tumour centre region. $*p < 0.05$

(0.89 ± 0.16 vs. 0.71 ± 0.15, [$p = 0.021$]), whereas no significant difference was found in the spleen between the two groups (embolization vs. sham, 1.26 ± 0.22 vs. 1.33 ± 0.23, [$p = 0.511$]) (Fig. 1b). The number of $CD8^+$T lymphocytes was comparable between groups in the spleen (Table S1, Fig. S3a, S3b). However, a significant decrease in the number of $CD8^+$T lymphocytes was detected in the TAE-treated tumours (113 ± 16 cells/mm^2 vs. 128 ± 13 cells/mm^2, [$p = 0.043$]). In detail, TAE treatment significantly reduced the recruitment of $CD8^+$T lymphocytes in the central regions (105 ± 22 cells/mm^2 vs. 126 ± 20 cells/mm^2, [$p = 0.045$]), but not in the marginal regions (124 ± 17 cells/mm^2 vs. 131 ± 7 cells/mm^2, [$p = 0.266$]) compared to sham-treated tumours (Fig. 2a, 2b). Furthermore, a greater number of $CD8^+$T lymphocytes were observed in the tumour marginal regions compared to central regions in TAE-treated tumours, whereas no such increase was observed in the sham-treated tumours (Table S1).

TAE Increased granzyme-B^+CD8^+ T Subtype Lymphocytes Infiltration in Tumour

When compared to the sham-treated rats, there was a tendency for greater proportion of PD-1^+CD8^+T lymphocytes in the spleens and tumours of TAE-treated rats (Table E1, Fig. S4a, S4b). The sham-treated tumours displayed a low frequency of granzyme-B^+CD8^+T lymphocytes infiltration at the tumour margin, tumour centre and the entire tumour. Furthermore, the distribution of granzyme-B^+CD8^+T lymphocytes was distributed evenly in both group of tumours (Fig. 3a, Fig. S5, Table S1). Notably, the percentage of granzyme-B^+CD8^+T lymphocytes in $CD8^+$T lymphocytes was significantly higher in the TAE-treated tumours compared to the sham-treated tumours (30.09% ± 7.70% vs. 22.20% ± 4.17%, [$p = 0.015$]), and this pattern was also evident in central regions (33.19% ± 8.17% vs. 24.11% ± 5.63%, [$p = 0.013$]) and marginal regions (25.06% ± 4.33% vs. 20.03% ± 4.03%, [$p = 0.020$]) (Fig. 3a, 3b). Furthermore, in tumours treated with TAE, a higher percentage of granzyme-B^+CD8^+T lymphocytes was observed in central regions, whereas this pattern was not evidenced in sham-treated tumours (Table S1, Fig. 3b).

TAE Increased Tumour PD-L1 Expression

The IHC results demonstrated no significant increase in the proportion of PD-1 positive areas in TAE-treated tumours in comparison with the sham-treated tumours (Table E1, Fig. S6a, S6b). In contract, the proportion of PD-L1 positive areas was considerable higher in the TAE-treated tumours when compared to the tumour margin(18.67% ± 5.43% vs. 13.59% ± 2.18%, [$p = 0.018$]), tumour centre (25.61% ± 8.01% vs. 15.05% ± 3.05%, [$p = 0.002$]) and entire tumour(22.53% ± 6.63% vs. 14.40% ± 1.43%, [$p = 0.002$]) (Fig. 4a, 4b). Compared to the homogeneous distribution of PD-L1 in the sham-treated tumours, the proportion of PD-L1 positive areas in the central regions of

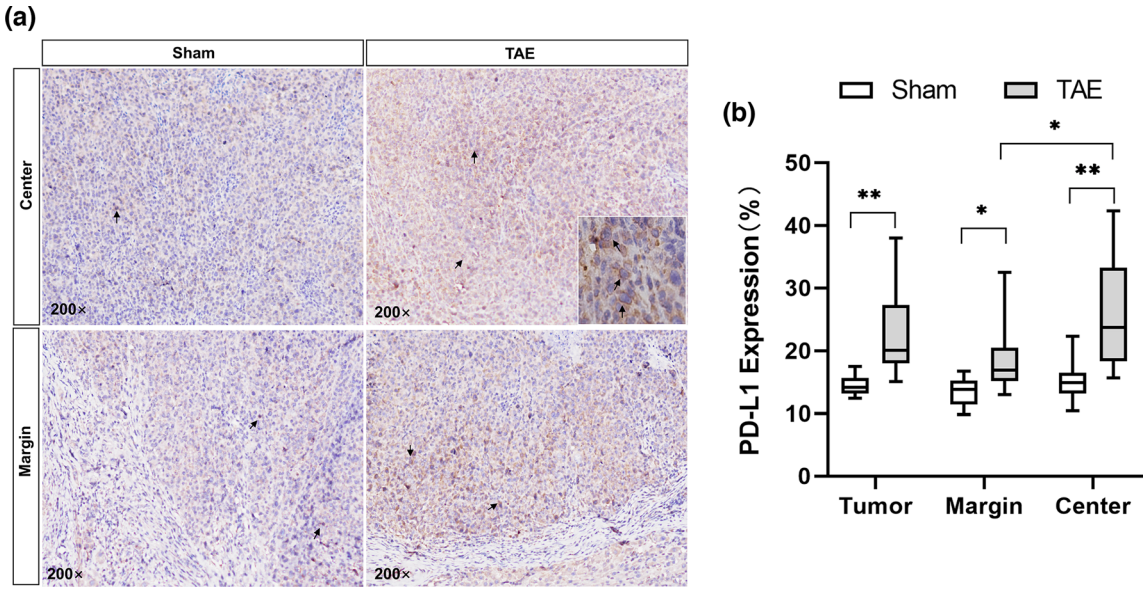

Fig. 4 The expression of PD-$L1^+$ cells in tumour tissues by IHC. **a** Representative IHC sections reveal PD-$L1^+$ cell (black arrows) with cell membrane staining (upper right magnified image). **b** Quantitative analysis shows a significant increase in PD-$L1^+$ cell expression in TAE-treated tumour tissue. The percentage of cell staining positive for PD-$L1^+$ is greatest in the centre of the tumour in the TAE group. *$p < 0.05$, **$p < 0.01$

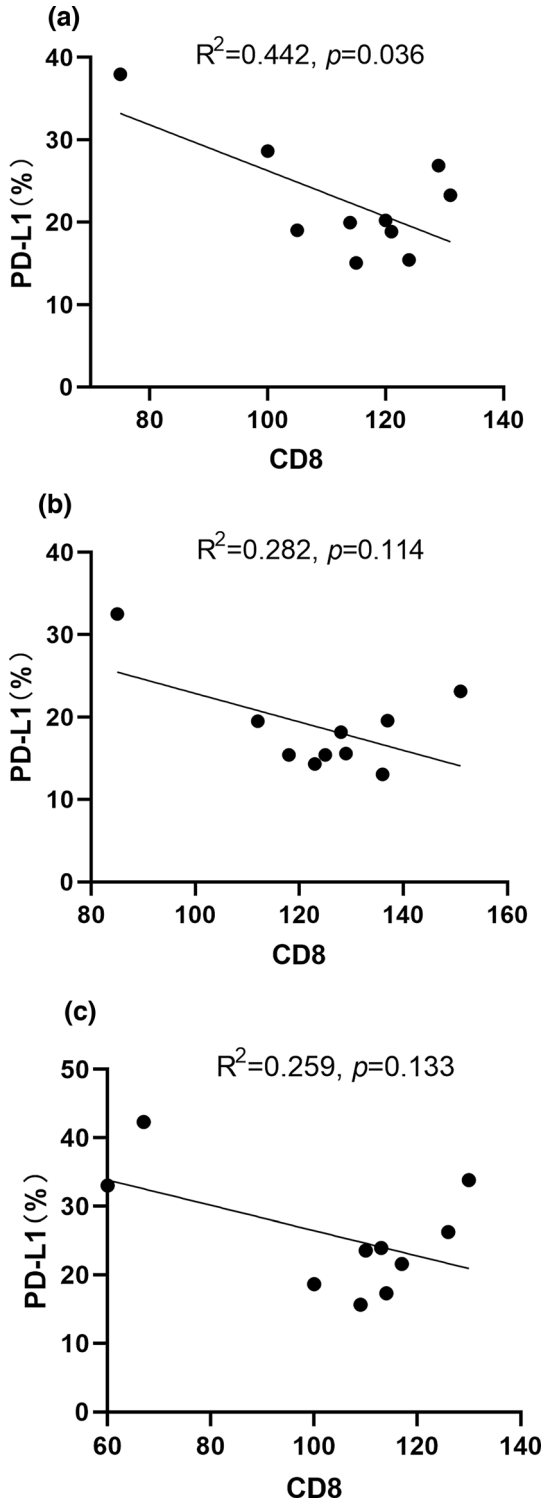

Fig. 5 The correlations between PD-L1 positive cells and $CD8^+$T lymphocytes infiltration on IHC in the TAE-treated tumours. **a** Correlation in overall tumours. **b** Correlation in the margins. **c** Correlation in the centres

the TAE-treated tumours was significantly higher (Table E1).

Relationship between $CD8^+$T infiltration and PD-L1 expression

Based on the results of IHC analysis that the number of $CD8^+$T lymphocytes infiltration and PD-L1 expression appeared to be conflicting, the potential relationship between the two variants was further explored in TAE-treated tumours. Interestingly, there was a negative correlation between the number of $CD8^+$T lymphocytes infiltrating and the percentage of PD-L1 positive areas in the entire tumours, marginal regions and central regions in TAE-treated tumours ($r^2 = 0.442$, [$p = 0.036$]; $r^2 = 0.282$, [$p = 0.114$] and $r^2 = 0.259$, [$p = 0.133$]; respectively) (Fig. 5a, 5b, 5c).

Discussion

While the integration of ICIs and anti-angiogenesis doubles tumour response rate compared to ICIs monotherapy; frequent drug resistance, lack of predictive biomarkers and severe adverse events result in approximately two-thirds of patients failing to response [18]. In this instance, locoregional therapy, which is believed to convert immunosuppressed HCC from a "cold" to a "hot" form, combined with ICIs is attracting considerable attention [19]. However, the stimulatory effect of TACE on immunoactivation has to be re-examined in the absence of substantial pathological evidence. While TACE-induced tumour necrosis and antigen release contribute to immunoactivation, the simultaneous hypoxia, inflammatory storm and accumulation of lactate ultimately lead to immunosuppression [20, 21].

The exacerbated PD-L1 in tumour tissues indicate that the timely integration of anti-PD-1/PD-L1 poses reasonable salvages to reverse immunosuppression after embolization and blocking potential immune escape [22]. Interestingly, an uneven spatial distribution of PD-L1 expression is observed in the TAE-treated tumours, with central regions exhibiting significantly higher PD-L1 levels than margins. Previous studies have demonstrated that the margins of HCC are less amenable to embolization than its central regions [23, 24]. Therefore, it is conceivable that hypoxia inducible factor-α may enhance PD-L1 expression moderately in tumour margins in comparison with the central areas. Furthermore, the infiltration of suppressive immune cells induced by inflammation and caused by necrosis may be more pronounced in tumour centre, and may eventually promote the expression of PD-L1 [21].

Although combination with anti-PD-1/PD-L1 following embolization represents a reasonable approach, the findings of this study do not yet support the hypothesis of a strong synergy between the two treatments. The results of this animal study offer insight into the outcomes of the EMERALD-1 trial, which demonstrated that TACE combined with durvalumab monotherapy is not clinically meaningful, while the addition of anti-angiogenesis significantly improved patient progression-free survival [25]. The decreased number of $CD8^+$T lymphocytes and the overexpression of PD-L1 following embolization define tumour status as intrinsic induction, which is incapable of optimizing ICIs response, even when exhausted $CD8^+$T lymphocytes are liberated by anti-PD-1/PD-L1 [11]. Additional interventions are required to facilitate the preliminary recruitment of $CD8^+$T lymphocytes and subsequent transfer of tumour status into the adaptive immune resistance [26, 27]. Subsequently, anti-PD-1/PD-L1 is expected with the objective of wakening $CD8^+$T lymphocytes to maximize immune response. Particularly, the distribution of $CD8^+$T lymphocytes in the tumour centre versus the tumour margin depicts a landscape similar to immune excluded, whereby CTLs are excluded from the actual cancer cell nests [28]. Tan et al. suggested that post-TACE accumulation of M2 macrophages within the TIME hinder $CD8^+$T recruitment [21]. High expression of PD-1/PD-L1 promotes $CD8^+$T lymphocytes apoptosis and vice versa [29]. This may have contributed to the observed negative association on $CD8^+$T lymphocytes infiltration and PD-L1 expression.

Embolization-induced hypoxia has long been considered as stumbling blocks to immune stimulation, whereas recent insights into metabolism find that hypoxia actually plays a necessary role in $CD8^+$T lymphocytes activity. Extracellular adenosine triphosphate released by dying cells, in an inflammatory context, is reported to enhance innate immunocytes, which in turn stimulates $CD8^+$T lymphocytes cytotoxicity theoretically [30–32]. This may explain the increased ratio of granzyme-B^+CD8^+T lymphocytes observed in TAE-treated tumours.

The evaluation of tumour immunity through simplified indicators is a relatively straightforward process; however, this approach is challenging to provide a comprehensive understanding of the subject. Notably, cytokines play a crucial role in the shaping of TIME within the tumour-immunity cycle [33]. Interleukin-6(IL-6) is intimately associated with the inflammatory TIME after embolization, as it serves as the primary mediator of pro-inflammatory signalling [34, 35]. The high expression of IL-6 not only accelerates tumour proliferation, but also enhances angiogenesis and enhances HCC stemness [36]. In particular, the negative relationship between IL-6 expression and anti-PD-L1 and anti-angiogenes is response highlights the necessity for further investigation into the optimal timing for combination therapy, with the objective of avoiding the immunosuppression induced by inflammation following embolization [37]. Furthermore, it has been proposed that the cytokine TGF-β may be employed as an additional indicator for tumour immunophenotyping [38]. In addition, several questions pertaining to immunology remain unanswered, including whether alterations in immune cells and immune checkpoints are associated with embolization materials and the impact of anti-angiogenesis prior to or following embolization on the TIME.

There are limitations in this study that require further explanation. First, this study carries limitations as it examines only a narrow range of phenotypes limited by the availability of suitable commercial antibodies. Second, the study solely explores the effects of embolization on immunity, while the impact of chemotherapeutic agents on $CD8^+$T and PD-1/PD-L1 falls outside the realm of this investigation. Finally, this study primarily concentrates on the short-term immune response of embolization on HCC. Future observations at multiple time points are needed to reveal dynamic changes in tumour immune status.

In conclusion, the results of this animal study indicate that the intrinsic induction status of the tumour in the short period after embolization is insufficient to elicit a maximal response to PD-1/PD-L1 inhibitors, based on the observation of a decreased number of $CD8^+$T lymphocytes and increased PD-L1 expression after TAE.

Funding This study was supported by the Natural Science Foundation of Jiangsu Province (SBK2023022210), and the Jiangsu Provincial Key Research and Development (BE2021648). Funding sources had no involvement in the financial support for the conduct of the research and preparation of the article.

Declarations

Conflict of interest On behalf of all authors, the corresponding author states that there is no conflict of interest.

Ethical approval All applicable international, national and/or institutional guidelines for the care and use of animals were followed. All procedures performed in studies involving animals were in accordance with the ethical standards of the institution at which the studies were conducted. This manuscript does not contain any studies with human participants performed by any of the authors.

Consent for Publication For this type of study, consent for publication is not required.

Informed Consent Animal experiments were approved by the Institutional Animal Care and Use Committee and conducted in accordance with the guidelines for animal experiments and related activities of the Laboratory Animal Center of Soochow University (approval serial number: 202306A0675).

References

1. Lencioni R, de Baere T, Soulen MC, Rilling WS, Geschwind JF. Lipiodol transarterial chemoembolization for hepatocellular carcinoma: a systematic review of efficacy and safety data. Hepatology. 2016;64:106–16.
2. Reig M, Forner A, Rimola J, et al. BCLC strategy for prognosis prediction and treatment recommendation: the 2022 update. J Hepatol. 2022;76:681–93.
3. Huang JT, Zhong BY, Jiang N, et al. Transarterial chemoembolization combined with immune checkpoint inhibitors plus tyrosine kinase inhibitors versus immune checkpoint inhibitors plus tyrosine kinase inhibitors for advanced hepatocellular carcinoma. J Hepatocell Carcinoma. 2022;9:1217–28.
4. Yang F, Yang J, Xiang W, et al. Safety and efficacy of transarterial chemoembolization combined with immune checkpoint inhibitors and tyrosine kinase inhibitors for hepatocellular carcinoma. Front Oncol. 2021;11: 657512.
5. El-Khoueiry AB, Llovet JM, Vogel A, et al. LEAP-012 trial in progress: Transarterial chemoembolization (TACE) with or without lenvatinib plus pembrolizumab for intermediate-stage hepatocellular carcinoma (HCC). Journal of Clinical Oncology. 2022;40(4):TPS494-94.
6. Zhu HD, Li HL, Huang MS, et al. Transarterial chemoembolization with PD-(L)1 inhibitors plus molecular targeted therapies for hepatocellular carcinoma (CHANCE001). Signal Transduct Target Ther. 2023;8:58.
7. Galon J, Bruni D. Approaches to treat immune hot, altered and cold tumours with combination immunotherapies. Nat Rev Drug Discov. 2019;18:197–18.
8. Schobert IT, Savic LJ, Chapiro J, et al. Neutrophil-to-lymphocyte and platelet-to-lymphocyte ratios as predictors of tumor response in hepatocellular carcinoma after DEB-TACE. Eur Radiol. 2020;30:5663–73.
9. Mocan T, Ilies M, Nenu I, et al. Serum levels of soluble programmed death-ligand 1 (sPD-L1): a possible biomarker in predicting post-treatment outcomes in patients with early hepatocellular carcinoma. Int Immunopharmacol. 2021;94: 107467.
10. Zhou G, Sprengers D, Boor PPC, et al. Antibodies Against Immune Checkpoint Molecules Restore Functions of Tumor-Infiltrating T Cells in Hepatocellular Carcinomas. Gastroenterology. 2017;153:1107-19e10.
11. Teng MW, Ngiow SF, Ribas A, Smyth MJ. Classifying cancers based on T-cell infiltration and PD-L1. Cancer Res. 2015;75:2139–45.
12. Craciun L, de Wind R, Demetter P, et al. Retrospective analysis of the immunogenic effects of intra-arterial locoregional therapies in hepatocellular carcinoma: a rationale for combining selective internal radiation therapy (SIRT) and immunotherapy. BMC Cancer. 2020;20:135.
13. Montasser A, Beaufrere A, Cauchy F, et al. Transarterial chemoembolisation enhances programmed death-1 and programmed death-ligand 1 expression in hepatocellular carcinoma. Histopathology. 2021;79:36–46.
14. Pinato DJ, Murray SM, Forner A, et al. Trans-arterial chemoembolization as a loco-regional inducer of immunogenic cell death in hepatocellular carcinoma: implications for immunotherapy. J Immunother Cancer. 2021;9(9):e003311.
15. Tischfield DJ, Gurevich A, Johnson O, et al. Transarterial embolization modulates the immune response within target and nontarget hepatocellular carcinomas in a rat model. Radiology. 2022;303:215–25.
16. Ueshima E, Sofue K, Takaki H, et al. Lenvatinib mitigates transarterial embolization-induced polarization of tumor-associated macrophages in a rat hepatocellular carcinoma model. J Vasc Interv Radiol. 2023;34(1977–85): e4.
17. Buijs M, Geschwind JF, Syed LH, et al. Spontaneous tumor regression in a syngeneic rat model of liver cancer: implications for survival studies. J Vasc Interv Radiol. 2012;23:1685–91.
18. Pinter M, Jain RK, Duda DG. The current landscape of immune checkpoint blockade in hepatocellular carcinoma: a review. JAMA Oncol. 2021;7:113–23.
19. Greten TF, Mauda-Havakuk M, Heinrich B, Korangy F, Wood BJ. Combined locoregional-immunotherapy for liver cancer. J Hepatol. 2019;70:999–07.
20. Xue TC, Jia QA, Ge NL, Chen Y, Zhang BH, Ye SL. Imbalance in systemic inflammation and immune response following transarterial chemoembolization potentially increases metastatic risk in huge hepatocellular carcinoma. Tumour Biol. 2015;36:8797–03.
21. Tan J, Fan W, Liu T, et al. TREM2(+) macrophages suppress CD8(+) T-cell infiltration after transarterial chemoembolisation in hepatocellular carcinoma. J Hepatol. 2023;79:126–40.
22. Peng Z, Fan W, Zhu B, et al. Lenvatinib combined with transarterial chemoembolization as first-line treatment for advanced hepatocellular carcinoma: a phase III. Randomized Clinical Trial (LAUNCH). 2023;41:117–27.
23. Takaki H, Hirata Y, Ueshima E, et al. Hepatic artery embolization enhances expression of programmed cell death 1 ligand 1 in an orthotopic rat hepatocellular carcinoma model in vivo and in vitro experimentation. J Vasc Interv Radiol. 2020;31(9):1475–82.
24. Miyayama S, Matsui O, Zen Y, et al. Portal blood supply to locally progressed hepatocellular carcinoma after transcatheter arterial chemoembolization: observation on CT during arterial portography. Hepatol Res. 2011;41:853–66.
25. Lencioni R, Kudo M, Erinjeri J, et al. 2024. EMERALD-1 A phase 3 randomized placebo-controlled study of transarterial chemoembolization combined with durvalumab with or without bevacizumab in participants with unresectable hepatocellular carcinoma eligible for embolization. 42: LBA432
26. Kudo M. Lenvatinib May Drastically Change the Treatment Landscape of Hepatocellular Carcinoma. Liver Cancer. 2018;7:1–19.
27. Kudo M. Limited Impact of Anti-PD-1/PD-L1 Monotherapy for Hepatocellular Carcinoma. Liver Cancer. 2020;9:629–39.
28. Mellman I, Chen DS, Powles T, Turley SJ. The cancer-immunity cycle: Indication, genotype, and immunotype. Immunity. 2023;56:2188–205.
29. Shi F, Shi M, Zeng Z, et al. PD-1 and PD-L1 upregulation promotes CD8(+) T-cell apoptosis and postoperative recurrence in hepatocellular carcinoma patients. Int J Cancer. 2011;128:887–96.
30. Doedens AL, Phan AT, Stradner MH, et al. Hypoxia-inducible factors enhance the effector responses of CD8(+) T cells to persistent antigen. Nat Immunol. 2013;14:1173–82.
31. Vuillefroy de Silly R, Ducimetiere L, Yacoub Maroun C, Dietrich PY, Derouazi M, Walker PR. Phenotypic switch of CD8(+) T cells reactivated under hypoxia toward IL-10 secreting, poorly proliferative effector cells. Eur J Immunol. 2015;45:2263–75.
32. Gropper Y, Feferman T, Shalit T, Salame TM, Porat Z, Shakhar G. Culturing CTLs under hypoxic conditions enhances their cytolysis and improves their anti-tumor function. Cell Rep. 2017;20:2547–55.
33. Propper DJ, Balkwill FR. Harnessing cytokines and chemokines for cancer therapy. Nat Rev Clin Oncol. 2022;19:237–53.
34. Yang YM, Kim SY, Seki E. Inflammation and liver cancer: molecular mechanisms and therapeutic targets. Semin Liver Dis. 2019;39:26–42.

35. Lokau J, Schoeder V, Haybaeck J, Garbers C. Jak-stat signaling induced by interleukin-6 family cytokines in hepatocellular carcinoma. Cancers (Basel). 2019;11(11):1704.
36. Xu J, Lin H, Wu G, Zhu M, Li M. IL-6/STAT3 is a promising therapeutic target for hepatocellular carcinoma. Front Oncol. 2021;11: 760971.
37. Yang H, Kang B, Ha Y, et al. High serum IL-6 correlates with reduced clinical benefit of atezolizumab and bevacizumab in unresectable hepatocellular carcinoma. JHEP Rep. 2023;5: 100672.
38. Montironi C, Castet F, Haber PK, et al. Inflamed and non-inflamed classes of HCC: a revised immunogenomic classification. Gut. 2023;72:129–40.